18th Brazilian Congress of Thermal Sciences and Engineering
November 16-20, 2020 (Online)

# ENC-2020-0033
# THE EFFECT OF THE PIPE ROUGHNESS ON THE TRANSIENT TURBULENT FLOW IN PIPES

**Douglas Monteiro Andrade**
**Felipe Bastos de Freitas Rachid**
Laboratory of Theoretical and Applied Mechanics – Mechanical Engineering Department – Universidade Federal Fluminense, Rua Rua Passo da Pátria, 156 – 246210-240 Niterói, RJ – Brazil
e-mails: dmajnj@gmail.com, rachid@vm.uff.br

***Abstract.*** *Pressure surges during pipe transient flow are important to the design and maintenance of the pipeline structure. This work argues about the effect of the pipe roughness on them. The analysis is carried out by the computed responses of a robust one-dimensional mechanical model of turbulent pipe flows. The pipe roughness is found to be relevant as pressures responses differ considerably. Such influence is herein justified by the fact of the pipe roughness generates different turbulent viscosity structures which are substantial to the overall fluid transient behavior.*

***Keywords:*** *fluid transient, transient friction, pipe roughness, turbulent flow*

## 1. INTRODUCTION

Transient turbulent flow is generated by abnormal and current daily operations in pipelines. Beyond being present in the industry, a major concern about these flows is caused by the appearances of larger pressure loads than those found in the steady regime. For that reason, the transient pressure responses must be employed as a crucial input to the development of safe pipeline projects. Yet this procedure is central, the rising pressures in fluid transients might change in the course of the operational time of the pipeline. The action of the conveyed fluid upon the pipe-walls affects its characteristics, as a result, the pressure field responds differently to the new overall fluid-pipe system (Covas, 2003). Therefore, the knowledge of the real impact of the pipe-wall features might be relevant to conserve pipeline integrity. This work arises to improve the understanding of this process by analyzing the influence of the pipe roughness on pipe transients.

To set a strategy for analyzing the influence of this parameter, first, a mechanical model that is capable of foreseeing with accuracy the behavior of the unsteady flow is a need. The nature of the transient flows differs drastically from the steady flow by the surge of adverse velocity gradients in regions next to the wall(Brunone et al., 2000). This characteristic turns the use of the same friction equation applied in steady state inaccurate when a precise description of transient flow is sought (Vítkovský et al., 2006).

Thus, modeling the transient requires more powerful transient friction models. A diverse range of models has been developed since the mid of the last century (Ghidaoui et al., 2005). Despite this vast literature, this work invokes a recent one-dimensional model proposed by Andrade(2018). This model achieves great compatibility with data from experiments. In addition, though this model is, in essence, one-dimensional, it is capable of describing not just the average pressure and velocity fields but also the velocity and shear profiles of the flow (Andrade, 2018). Moreover, the material constants of the model are lightly computed, depending on the initial Reynolds number and pipe roughness of the pipe. Thus, the analysis of the main variable of this work is made straightforwardly.

Taking advantage of this vast capacity, this transient friction (Andrade, 2018) is applied herein to make this preliminary theoretical analysis of the pipe roughness effects upon turbulent transients. Computations of the same transient flow but pipe roughness are performed to see the importance of this parameter in fluid transient responses. The analysis is not restricted to the pressure traces, on the contrary, the assertions have a significant appeal to the transient responses of mean velocity, velocity profile and shear stress.

## 2. MECHANICAL MODEL

The one-dimensional transient friction model of Andrade (2018) is based on the Theory of Mixture mathematical framework. In this context, the mixture is formed by $n$ isothermal constituents which one within its own kinematics. Nevertheless, instead of being composed of perfectly blended constituents, in the work of Andrade (2018), the mixture is envisaged by a set of structured shell-shaped constituents as they are pseudo-layers of the fluid flow as shown in Fig. 1. As one can see, each one of these mixture components is characterized by its radius $R_j$ and thickness $\Delta R_j$ which are computed by

$$R_j == R_{j-1} + \Delta R_j, \tag{1}$$

$$\Delta R_j = \frac{R}{n}, \tag{2}$$

respectively, in addition to a fixed volumetric fraction given by

$$\alpha_j = \frac{2R_j \Delta R_j}{R^2}, \text{ for } \quad j = 1,..n. \tag{3}$$

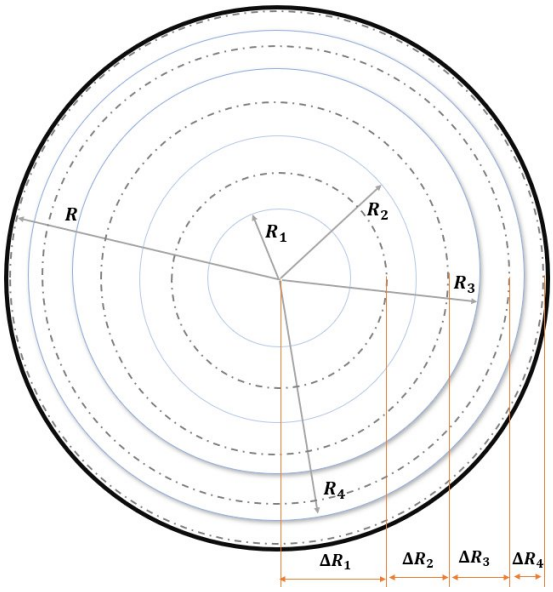


Figure 1. Virtual structured of the mixture for $n = 4$.

Assuming that the gravitational effects may be neglected and that a barotropic fluid flows at low Mach number inside a pipe bearing linear elastic deformations; the local form of the mechanical balances that govern the transient flow may be expressed as (Andrade, 2018)

$$\frac{1}{a^2}\frac{\partial p}{dt} + \rho \frac{\partial v}{\partial x} = 0, \tag{4}$$

$$\rho \frac{\partial v}{\partial t} + \frac{\partial p}{\partial x} + \frac{2}{R}\sum_{j=1}^{n} a_j = 0, \tag{5}$$

$$\alpha_j \rho \frac{\partial v_j}{\partial t} + \alpha_j \frac{\partial p}{\partial x} + m_j + \frac{2}{R} a_j = 0, \quad j = 1,..., n \tag{6}$$

In which the mass and momentum for the mixture as a whole are represented by the Eq. (4) and Eq. (5), respectively, whilst the momentum for each constituent of the virtual mixture is represented by the Eq. (6). In those equations, $a$ is the wavefront velocity, and the velocity and density of the mixture as a whole are represented by $v, \rho$ meanwhile $v_j$, $\rho_j$ represent these features for the *j-th* constituent of the mixture. In addition, $m_j$ is the internal interaction force per unit of cross-sectional area exerted by the other constituents on the *j-th* constituent, and $a_j$ is the reactive contact friction force per unit lateral area that acts on the pipe wall-fluid interface.

These aforementioned mechanical forces are addressed by appealing to the objectivity principle and kinematic aspects of the structured mixture, and are given by Andrade (2018):

$$m_j = C_{j,j-1}\left(v_j - v_{j-1}\right) + C_{j,j+1}\left(v_j - v_{j+1}\right), \tag{7}$$

for $j = 1,\ldots, n-1$,

$$a_j = \begin{cases} 0, & for\ j = 1,\ldots, n-1 \\ Cv_n, & for\ j = n \end{cases}, \tag{8}$$

in which $C_{j,j+1}$ , $C_{j,j-1}$, $C$ are the thermomechanical constants of the model.

Them material constants are obtained assuming that the turbulent viscosity distribution does not change during the transient. With this assumption and with the calling of a steady-state turbulent velocity profile, such constants turn to be the solution of a linear system formed by the set of momentum equations of each constituent in steady-state.

The selected velocity profile is based on a turbulent viscosity distribution in which a core region ($0 < r < 0.8R$) has a constant valued kinematic viscosity $\nu_c$ while in the annulus region ($0.8 < r < R$), the viscosity has a linear descendent behavior towards the wall viscosity $\nu_w$. Both viscosities are functions of the initial Reynolds number and pipe roughness and may be found with the Darcy-Weisbach formulas of friction factor (Vardy & Brown, 2007).

This strategy leads to core material constants that may be presented as

$$C_{j,j+1} = \frac{4\rho\nu_c}{R_{j+1}^2 - R_j^2}\left(\sum_{i=1}^{j}\alpha_i\right) \tag{9}$$

and annular material constants of

$$C_{j,j-1} = \frac{2\nu_w\rho(1-\sigma_{cw})}{b^2\left\{\dfrac{R_{j+1}-R_j}{b} + \dfrac{\left(-4+5\sigma_{cw}\right)}{\left(1-\sigma_{cw}\right)}\ln\left[\dfrac{\left(\dfrac{1-\sigma_{cw}}{b}\right)R_j - 4 + 5\sigma_{cw}}{\left(\dfrac{1-\sigma_{cw}}{b}\right)R_{j+1} - 4 + 5\sigma_{cw}}\right]\right\}}\left(\sum_{i=1}^{j}\alpha_i\right). \tag{10}$$

At last, the pipe-fluid interface material constant achieves the form of

$$C = \frac{\nu_w\rho R\left(1-\sigma_{cw}\right)}{b^2\left\{\dfrac{R-R_n}{b} + \dfrac{\left(-4+5\sigma_{cw}\right)}{\left(1-\sigma_{cw}\right)}\ln\left[\left(\dfrac{1-\sigma_{cw}}{b}\right)R_n - 4 + 5\sigma_{cw}\right]\right\}}\left(\sum_{i=1}^{n}\alpha_i\right). \tag{11}$$

In Eq. (10) and Eq. (11), $\sigma_{cw}$ stands for the ratio of core and wall viscosities and $b$ represents the annular thickness meaning $0.2R$.

Note that, yet the model is virtually one-dimension, not just the average pressure and velocity are achieved by solving Eqs. (4, 5, 6), but also the fluid velocity profile, that is the assemble of the velocities of the mixture constituents. Basically, this discrete grid of constituents forms a discrete form of computing the momentum flux, in which the shear stress for the *j-th* constituent may be interpreted in the presented mechanical model as

$$\tau_j = \begin{cases} \dfrac{R_j}{2}\left[C_{j,j+1}\left(v_j - v_{j+1}\right)\right], & \text{for } j = 1, n-1 \\ a_n & \text{for } j = n. \end{cases} \tag{12}$$

As the mechanical model is completely described, we now present the numerical procedure. In this work, the classic method of characteristics is applied to solve the mechanical model with the aid of a Crank-Nicolson approximation of constituent interaction forces $a_j$ and $m_j$. Further, the spatial grid of the method of characteristics is established to have 41 nodes while the number of constituents applied herein is 80.

## 3. VALIDATION OF THE MODEL

To validate the model, the experimental data from Adamkowski & Lewandowski (2006) is used. Their apparatus was the classic reservoir-pipe-valve setup (see Fig. 2), in which transient flow arises from a rapid closure valve maneuver meanwhile the reservoir is maintained with a constant pressure. The boundary conditions of such setup may be modeled as

$$p(x = 0, t) = p_0, \tag{13}$$

$$v(L, t) = \begin{cases} v_0\left(1 - \dfrac{t}{t_c}\right) & \text{if } 0 \le t < t_c \\ 0 & \text{if } t \ge t_c \end{cases} \text{ for closure; and} \tag{14}$$

in which $t_c = 0.003s$ is the valve closure time, $p_0$ stands for the reservoir pressure and $v_0$ represents the initial velocity. This experiment was carried out with water ( $\rho = 1000\ Kg/m^3$ and $\nu = 9.49 \times 10^{-7}$ ) at Reynolds number of 5731 which flows in a pipe of $98.11m$ of length $L$ and internal diameter of $0.016\ m$. The pipe relative roughness and wave-speed were stated to be 0.000438 and 1301.8 *m/s,* respectively (Gonzaga Filho, 2017). A sketch of the experimental apparatus is shown in Fig. 2.

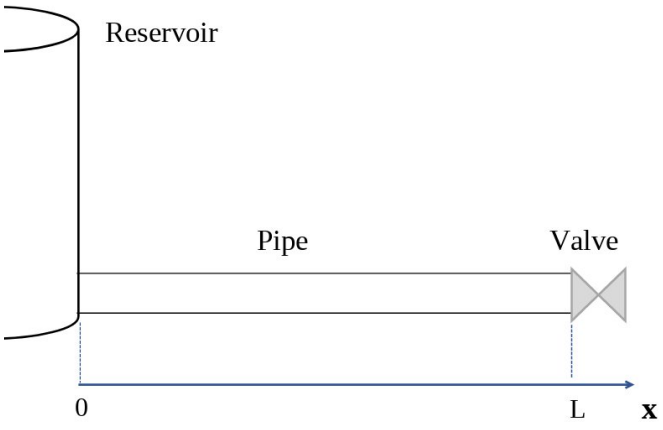


Figure 2. Sketch of the test rig used in the experiments whose data will be used for validating the model.

The results throughout this work are normalized for a better visualization of the phenomenon. Water-hammer time scale $t^* \equiv L/a$ is invoked to normalize the time whereas mean velocity, shear stress are normalized by their steady state counterparts $V_0$, $\tau_{w0}$. Pressure responses are shown as the difference between the computed head and its related

steady state value $\Delta H \equiv H - H_0$ normalized by the Joukowsky head $H^*$. Such pressure is defined as $H^* \equiv av_0/g$ where $g$ means gravity.

The dimensionless head responses computed by the present model and the Adamkowski and Levandowski (2006) data are presented in Fig. 3. As one can note, the model attains a good agreement with the experiment. Besides pressure, the average velocity, wall shear stress and rate of energy dissipation of transient flow were also performed in Andrade (2018). By means of theoretical analysis and comparison to other friction models of literature, this work demonstrates that such variables also are computed accurately. What turns its model to be solid enough for further usage in transient analysis when these features are key-rollers.

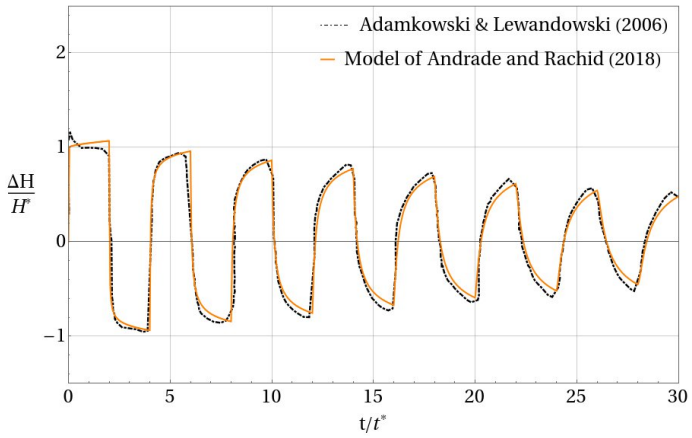


Figure 3. Normalized head time history at the valve location in the Adamkowski & Lewandowski (2006) experiment compared to the responses of the model of Andrade (2018).

## 4. ANALYSIS OF THE INFLUENCE OF THE PIPE ROUGHNESS

The effect of the pipe roughness in transient flow responses is observed by choosing three different values of this parameter to replace the one of the experiment of Adamkowski and Levandowski (2006). Case 1 represents a smooth-walled pipe, and the subsequent cases present two different relative roughness which are capable of increasing significantly the Darcy-Weisbach friction factor, being Case 3 the roughest case. The change in the pipe roughness influences directly in the friction factor and viscosity structure of the model (Vardy and Brown, 2007). In Table 1, one can find a summary of the three different cases in terms of these features. One may note that the turbulent viscosity structure is highly influenced by the pipe roughness. The turbulent wall viscosity is the most affected ranging from its molecular value to six-time higher than that.

Table 1. Cases studied

| | $\epsilon$ | $f$ | $\nu_c \left(\frac{m^2}{s}\right)[10^{-6}]$ | $\nu_w \left(\frac{m^2}{s}\right)[10^{-6}]$ |
|---|---|---|---|---|
| Case 1 | 0.00 | 0.036 | 5.42 | 0.949 |
| Case 2 | 0.02 | 0.054 | 6.68 | 2.2387 |
| Case 3 | 0.08 | 0.093 | 9.31 | 6.5015 |

The pressure responses at the pipe-midlength for the three cases are shown in Fig. 4. Observe that in the first cycle, all case have the pressure superior to the Joukowsky head, which is a phenomenon known in the literature as linepacking. One can note that the pipe roughness drives this phenomenon to be more pronounced. However, the same cannot be said to the latter stages of the transient because of the stronger pressure attenuation in rough-walled pipes. Therefore, in a certain way, the overall cyclic pressure load is less severe and works to the safer side of the pipeline integrity.

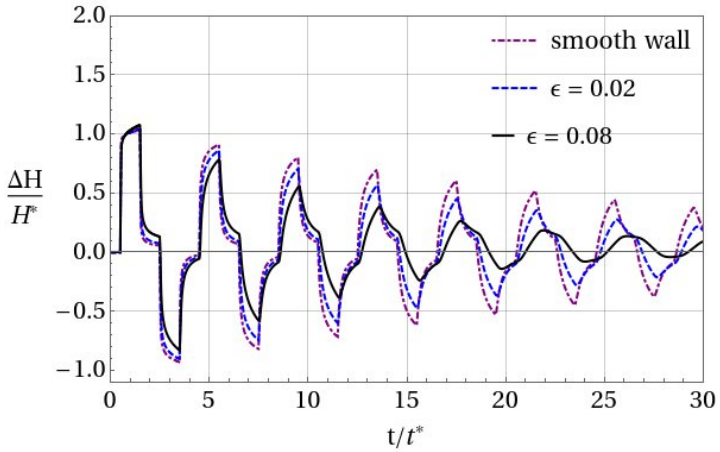


Figure 4. Normalized head at the mid-length of the pipe versus time at the valve predicted by the present model for different pipe roughness.

To better understand the phenomenon, one can observe the balance laws in the compatibility form (Andrade, 2018), in which the hyperbolic partial differential system is transformed into a system of ordinary differential equations along with their characteristics

$$\frac{1}{a}\frac{dp}{dt} = \left(\rho_0 \frac{dv}{dt}\right) + \left(\frac{2}{R}\sum_{j=1}^{n} a_j\right), \quad \text{along } C^-: \frac{dx}{dt} = -a, \tag{15}$$

$$-\frac{1}{a}\frac{dp}{dt} = \left(\rho_0 \frac{dv}{dt}\right) + \left(\frac{2}{R}\sum_{j=1}^{n} a_j\right), \quad \text{along } C^+: \frac{dx}{dt} = +a \tag{16}$$

$$\left.\begin{array}{ccc} \frac{dv}{dt} = \frac{dv_2}{dt} - \frac{2}{\rho_0 R}\sum_{j=1}^{n} a_j + \frac{m_2 + \frac{2}{R}a_2}{\rho_0 \alpha_2} & & \\ \vdots \quad \vdots \quad \vdots & \vdots & \vdots \\ \frac{dv}{dt} = \frac{dv_n}{dt} - \frac{2}{R\rho_0}\sum_{j=1}^{n} a_j + \frac{m_n + \frac{2}{R}a_n}{\rho_0 \alpha_n} & & \end{array}\right\} \quad \text{along } C^0: \ \frac{dx}{dt} = 0, \tag{17}$$

This classical form infers that the closure of the valve gives rise to a wave which travels periodically in the pipe within the region of influence delimited by the characteristics of the system. The arrival of the wave at a certain location makes its pressure rises/decreases scaled by the wave velocity and balanced by the inertial and pipe-fluid interface forces (see Eqs. (15, 16)). In addition, both of these forces depend on the momentum diffusion between the pseudo-constituents of the mixture (Eq. 17). This complex relationship can be exposed by presenting the velocity profiles at midlength of the pipe in the first moments of the transient (see Fig. 5).

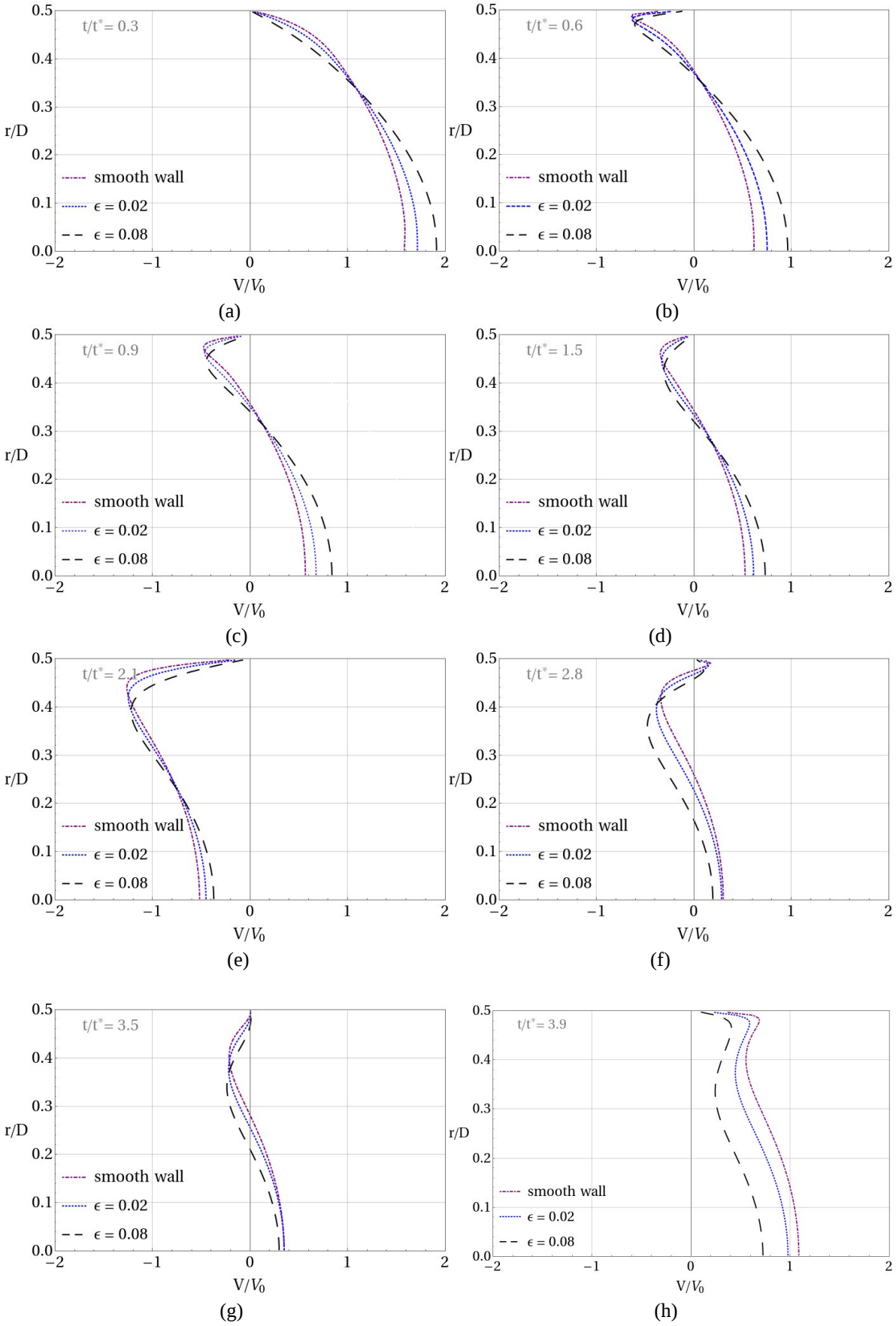


Figure 5. Normalized velocity profiles at the mid-length of the pipe predicted by the present model for different pipe roughness

First, it is perceptible that the different turbulent viscosity structure causes the steady state velocity profiles for different pipe roughness to be slightly different. The roughness in the wall makes the profile velocity to have minor velocity gradients at the wall while great values of velocity close to the center of the pipe. Right after the onset of the transient, the velocity gradients close to the wall are inverted but those found in more central regions remain positive. At this moment, the wall shear stress is extremely negative meanwhile the mean velocity is positive. In fact, as can be observed in Fig. 5 (b, c, d, f) aligned with Fig.6 (a, b), during several moments of the transient the wall shear stress and the average velocity are not in phase. Thus, the relation found in Eqs. (15, 16) is not trivial.

One may note that when the first wave arrives $\left(\frac{t}{t^*}=0.5\right)$ at the midlength of the pipe, the large negative velocity values close to the wall surges and shifts the signal of wall the shear stress in that region while the mean velocity is still positive for all cases (see Fig. 6). Nevertheless, the roughest wall case generates moderate velocity gradients (shear stress) and still conserves the most positive core velocities. This behavior makes the pressure to be greatest in such a case (see Eqs (15, 16) and Figs. 4, 5(b), 6). At the second wave arrival $\left(\frac{t}{t^*}=1.5\right)$, the velocity starts to shift completely its direction. The most accentuated negative velocities found in smooth walls make the lowest mean velocity, both acting to produce the smallest pressure ((see Eqs (15, 16) and Figs. 4, 5(e), 6).). When the third wavefront come into play $\left(\frac{t}{t^*}=2.5\right)$, the keen velocity gradients together with central greater core velocities turn the smooth case to be the less negative mean velocity. In a way that the pressure attains values nearer zero ((see Eqs (15, 16) and Figs. 4, 5(e, f), 6). Finally, the fourth wavefront $\left(\frac{t}{t^*}=3.5\right)$ inverts the direction of the flow again, where one can find the greatest velocities, wall shear stress and so the pressure in Case 1 ((see Eqs (15, 16) and Figs. 4, 5(g, h), 6).

The same logic can be extended over the cycles of the transient. In a way that the rougher walls will damp the velocity, wall shear stress and consequently the pressure during the transient.

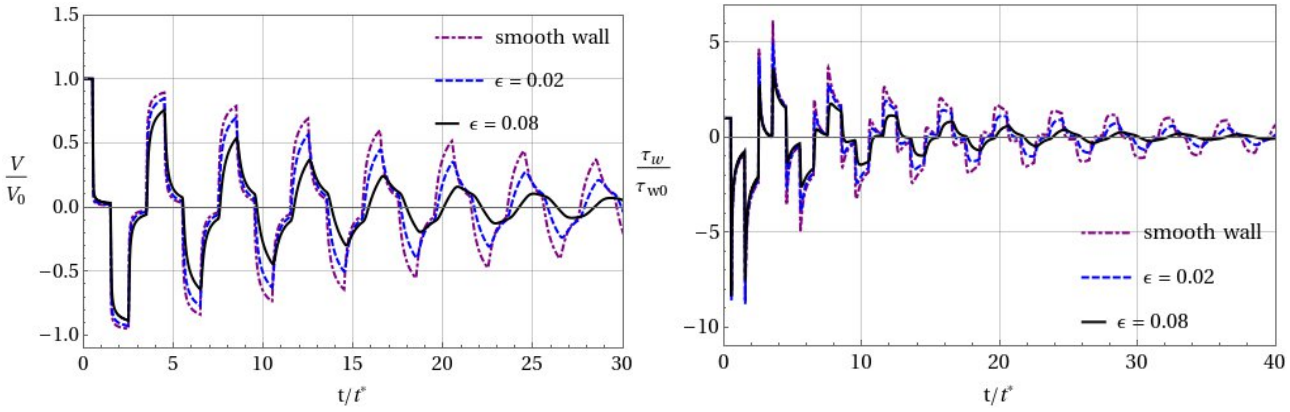


Figure 6. Normalized velocity (a) and shear stress (b) at the mid-length of the pipe predicted by the present model for different pipe roughness.

Throughout the description of the velocity profile through the passage of the waves, some behavior as the faster and more abrupt change of flow direction in the $t/t^* = 3.9$ for the smooth-walled case go farther than the slightly different found in the initial velocity profiles. The velocity profile in Case 1 seems to be the most affected by the cyclic pressure force bring it by the water hammer. Which in the end, turns the damping of the velocity and pressure slower than the other cases.

As the turbulent structure is assumed to be unchanged during the transient, the same material constants responsible for different initial velocity profiles also are the ones that give distinct velocity adjustments during the fluid transient. The momentum diffusion timescale from the wall towards central regions during unsteady pipe flows is given by (He. et al. 2008)

$$D_t \equiv \frac{2R}{\sqrt{\frac{\tau_{w0}}{\rho}}} = \frac{4\sqrt{2}\,R}{V_0\sqrt{f\left(\nu_w, \nu_c\right)}}. \tag{18}$$

As one can note from Eq. (18) together with Table 1, the increase in turbulence leads to faster momentum diffusion. Thus, in rougher walls, the momentum diffusion is rapidly enough to understand the new pressure gradient in such a way that attenuates more efficiently the inertial difference between the non-slip condition at the wall and more central regions of the flow. Furthermore, inner velocity gradients are rapidly influenced as can be seen over the subsequent actions of the wavefront (Fig. 5). This whole processing attains the set of mean velocity and shear stress described previously that produces the faster pressure damping. This fact is more evident when the shear stress profiles at the mid-pipe of Cases 1 and 3 at different stages of the transient are presented in Fig. 7. In the roughest case, the shear forces are present in more core flow regions before and after the outset of the transient. In addition, it seems that this phenomenon is more discernible as time pass.

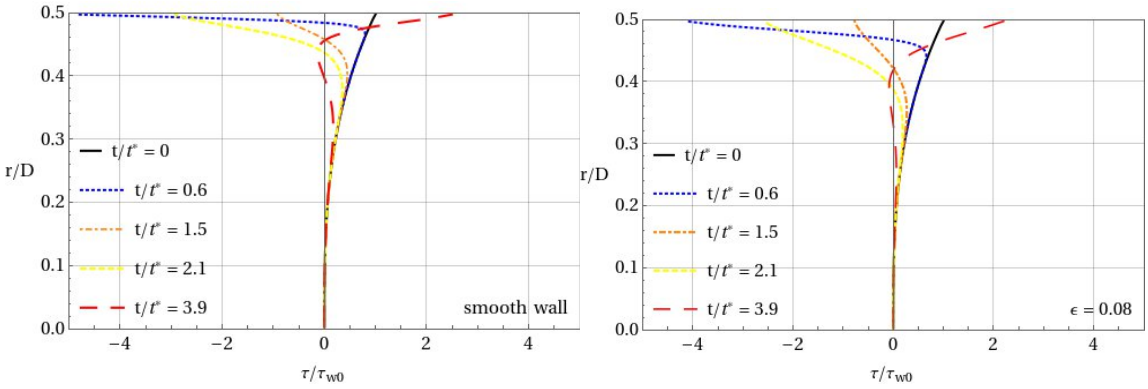


(a) (b)

Figure 7. Normalized shear stress profiles at the mid-length of the pipe predicted by the present model for case 1 (a) and case 3 (c).

## 5. CONCLUSION

An investigation of the pipe roughness in turbulent fluid transients is presented through the use of a mechanical model in which the transient friction is taken into account. The main effect caused by the increase of the roughness is the elevation of the pressure in the first cycle of the transient followed by stronger attenuation over the rest of the time span. This result can be useful for the construction and maintenance of safer pipelines.

The efficient turbulent mixing found in rougher walls eases the turbulent momentum diffusion from the wall towards the core flow during the fluid transient. This mechanism makes the average velocity and wall shear stress decrease strongly in time which leads to the damping of the pressure that is directly linked with those variables.

## 6. ACKNOWLEDGMENTS

The first author would like to gratefully thank the Brazilian agency CAPES for granting him financial support by means of a scholarship during his post-graduate course.

## 7. REFERENCES

Adamkowski, A., & Lewandowski, M. (2006). Experimental examination of unsteady friction models for transient pipe flow simulation. *Journal of Fluids Engineering, Transactions of the ASME*, *128*(6), 1351–1363. https://doi.org/10.1115/1.2354521

Andrade , D.M. (2019). *A model for transient friction in turbulent pipe flows based on the continuum theory of mixtures*. M.Sc. Dissertation, Universidade Federal Fluminense, Niterói, Brasil.

Brunone, B., Karney, B., Mecarelli, M., & Ferrante, M. (2000). Velocity Profiles and Unstead Pipe Friction in Transient Flow. *Journal of Water Resources Planning and Management*, *126*(4), 236–244.

Covas, D. I. C. (2003). Inverse transient analysis for leak detection and calibration of water pipe systems modelling special dynamics effects. *Imperial College of Science, Technology and Medicine, Civil and Environmental Engineering, PhD Thesis*, (January), 436.

Ghidaoui, M. S., Zhao, M., McInnis, D. A., & Axworthy, D. H. (2005). A Review of Water Hammer Theory and Practice. *Applied Mechanics Reviews*, *58*(1), 49. https://doi.org/10.1115/1.1828050

Gonzaga Filho, J. (2017). One evaluation of the models for describing friction in one-dimensional transient pipe flow. M.Sc. Dissertation. Graduate Program in Mechancial Engineering. Universidade Federal Fluminense, Niterói, Brazil. (In Portuguese).

He, S., Ariyaratne, C., & Vardy, A. E. (2008). A computational study of wall friction and turbulence dynamics in accelerating pipe flows. *Computers and Fluids*, *37*(6), 674–689. https://doi.org/10.1016/j.compfluid.2007.09.001

Pezzinga, G. (2000). Evaluation of Unsteady Flow Resistances by Quasi-2D or 1D Models. *Journal of Hydraulic Engineering*, *126*(10), 778–785. https://doi.org/10.1061/(ASCE)0733-9429(2000)126:10(778)

Vardy, A. E., & Brown, J. M. (2007). Approximation of Turbulent Wall Shear Stresses in Highly Transient Pipe Flows. *Journal of Hydraulic Engineering*, *133*(11), 1219–1228. https://doi.org/10.1061/(ASCE)0733-9429(2007)133:11(1219)

Vítkovský, J. P., Bergant, A., Simpson, A. R., & Lambert, M. F. (2006). Systematic Evaluation of One-Dimensional Unsteady Friction Models in Simple Pipelines. *Journal of Hydraulic Engineering*, *132*(7), 696–708. https://doi.org/10.1061/(ASCE)0733-9429(2006)132:7(696)

## 8. RESPONSIBILITY NOTICE

The author(s) is (are) the only responsible for the printed material included in this paper.